









Cite this: *Nanoscale*, 2018, **10**, 23113

Hydride-induced ligand dynamic and structural transformation of gold nanoclusters during a catalytic reaction†

Ricca Rahman Nasaruddin, ^{a,b} Qiaofeng Yao, ^a Tiankai Chen, ^a
Max J. Hülsey, ^a Ning Yan ^{*a} and Jianping Xie ^{*a}

Quasi-homogeneous ligand-protected gold nanoclusters (Au NCs) with atomic precision and well-defined structure offer great opportunity for exploring the catalytic nature of nanogold catalysts at a molecular level. Herein, using real-time electrospray ionization mass spectrometry (ESI-MS), we have successfully identified the desorption and re-adsorption of *p*-mercaptobenzoic acid (*p*-MBA) ligands from Au₂₅(*p*-MBA)₁₈ NC catalysts during the hydrogenation of 4-nitrophenol in solution. This ligand dynamic (desorption and re-adsorption) would initiate structural transformation of Au₂₅(*p*-MBA)₁₈ NC catalysts during the reaction, forming a mixture of smaller Au NCs (Au₂₃(*p*-MBA)₁₆ as the major species) at the beginning of catalytic reaction, which could further be transformed into larger Au NCs (Au₂₆(*p*-MBA)₁₉ as the major species). The adsorption of hydrides (from NaBH₄) is identified as the determining factor that could induce the ligand dynamic and structural transformation of NC catalysts. This study provides fundamental insights into the catalytic nature of Au NCs, including catalytic mechanism, active species and stability of Au NC catalysts during a catalytic reaction.

Received 4th September 2018,
Accepted 19th November 2018
DOI: 10.1039/c8nr07197g

rsc.li/nanoscale

1 Introduction

Ligand-protected gold nanoclusters (Au NCs) are metallic molecules or molecular-like metals, which find increasing acceptance in gold catalysis owing to their atomic precision, unique and well-defined molecular structure, ultrasmall size (~1 nm), and discrete electronic structure.^{1–3} With intact ligands on the surface, Au NCs could not only function as heterogeneous catalysts like gold nanoparticles (Au NPs, as the Au atoms in the core of Au NCs are mostly Au(0)), but also work as homogeneous metal–ligand complexes (*e.g.*, Au(I)-ligand or Au(III)-ligand, as the Au atoms in the staple motifs of Au NCs are mostly Au(I)).⁴ Therefore, ligand-protected Au NCs can also be regarded as quasi-homogeneous catalysts.^{5–7} Although Au NC catalysts have been studied in various chemical transformations, including oxidation,^{8–26} carbon–carbon

coupling reactions,^{27–29} hydrogenation,^{6,9,12,30–37} and electrochemical reactions,^{38,39} their catalytic nature such as the catalytic mechanism at molecular level and the actual active sites during a catalytic reaction are still ambiguous and not well understood. These aspects are rarely investigated, as in previous studies, Au NC catalysts were often transformed into heterogeneous catalysts and their ligands were removed, which might disrupt the atomic precision and well-defined structure of NC catalysts, further constraining the molecular-level understanding of their catalytic nature.^{19,26,40}

Recently, theoretical calculations have been used to reveal the active sites of Au NC catalysts. Taking Au₂₅(SR)₁₈ NC as an example (here SR denotes thiolate ligand), the active sites of Au NCs have been identified as the exposed (uncapped) Au₃ facets on the gold core, which are rich in electrons.^{6,12,35} The volcano-like structures of Au₃ facets have been reported as the active sites in catalytic reactions such as hydrogenation of cyclic ketones,³⁵ 4-nitrophenol,^{40,41} α,β-unsaturated ketones and aldehydes.⁶ Apart from the gold core, the low-coordinated Au atoms in the staple motifs were also reported as efficient catalytic active sites of Au NCs, especially for the association and activation of molecular hydrogen during the hydrogenation reaction.^{6,35} Interestingly, the activation of Au active sites at the staple motifs requires the removal of at least one ligand.^{27,28} For instance, based on density functional theory (DFT) calculation, the Au₂₅(SR)₁₈ NCs supported on cerium

^aDepartment of Chemical and Biomolecular Engineering, National University of Singapore, 4 Engineering Drive 4, Singapore 117585, Singapore.

E-mail: ning.yan@nus.edu.sg, chexiej@nus.edu.sg

^bDepartment of Biotechnology Engineering, Kulliyah of Engineering, International Islamic University Malaysia, P.O. Box 10, 50728 Kuala Lumpur, Malaysia

†Electronic supplementary information (ESI) available: Detailed molecular formula and validation of identified species in ESI-MS analyses. See DOI: 10.1039/c8nr07197g

oxides ($\text{Au}_{25}(\text{SR})_{18}/\text{CeO}_2$) can efficiently catalyze the Ullmann hetero-coupling reaction after exposing the low-coordinated Au atoms by removing at least one thiolate ligand from the staple motifs.^{27,28} However, the Au NC catalysts were deposited on metal oxides, and the detailed information on the structure of the Au NCs after the removal of ligands was not clear.

The structural transformation of Au NCs is another important topic that can expand the scope of research on metal NCs. Several recent studies reported the structural transformation of Au NCs in reductive and oxidative environments. For example, upon addition of a strong oxidant, hydrogen peroxide (H_2O_2), $[\text{Au}_{23}(\text{SR})_{16}]^-$ was transformed into $[\text{Au}_{28}(\text{SR})_{20}]^0$.⁴² In another study, upon addition of a strong reductant, NaBH_4 , $[\text{Au}_{25}(\text{SeR})_{18}]^-$ (SeR denotes selenolate ligand) was transformed into $[\text{Au}_{23}(\text{SeR})_{16}]^-$.⁴³ These two studies mainly focused on the synthesis and characterization of Au NCs. We realized that exploring the structural transformation of Au NCs during catalytic reaction is encouraging and attractive because this study may provide better insights into the catalytic nature of Au NCs during a reaction.^{15,44} For instance, a recent study suggests that the structural transformation of $\text{Au}_{25}(\text{SR})_{18}$ in styrene oxidation had facilitated the understanding of the active sites and catalytic mechanism of Au NCs.⁴⁴ However, the structural transformation analysis was mainly based on DFT calculations. To the best of our knowledge, experimental investigation into the structural transformation of Au NCs during a catalytic reaction is presently lacking, especially for solution-based catalytic hydrogenation.

In this study, we have identified the ligand dynamic and structural transformation of thiolate-protected Au_{25} NC catalysts during the catalytic hydrogenation of 4-nitrophenol in solution. The catalytic activity and structural transformation of Au NCs during the reaction were analyzed by UV-Vis absorption spectrometry and electrospray ionization mass spectrometry (ESI-MS). Interestingly, we observed desorption and re-adsorption of *p*-mercaptobenzoic acid (*p*-MBA) ligands on the Au NC catalysts, as well as the formation of several new Au NC species from the structural transformation of $\text{Au}_{25}(\text{p-MBA})_{18}$ NCs during the catalytic reaction. The ligand dynamic and structural transformation were induced by the adsorption of hydrides (from NaBH_4), as suggested by ESI-MS data. These experimental evidences shed light on the catalytic nature of Au NC catalysts during the hydrogenation of 4-nitrophenol in solution, further highlighting the benefits of using ligand-protected atomically precise Au NCs as model gold catalysts to reveal catalytic mechanisms at a molecular level.

2 Experimental

Materials

All chemicals were commercially available and used without further purification. Gold(III) chloride trihydrate ($\text{HAuCl}_4 \cdot 3\text{H}_2\text{O}$), *p*-mercaptobenzoic acid (*p*-MBA) and 4-nitrophenol were purchased from Sigma-Aldrich. Sodium hydroxide (NaOH) and ethanol were purchased from Merck. Carbon

monoxide (CO) was provided by SOXAL. Ultrapure water (Milli-Q) with a resistivity of 18.2 M Ω was used as the solvent for the synthesis and the catalytic reactions.

Preparation and characterization of Au NC catalyst

Synthesis of *p*-MBA-protected $\text{Au}_{25}(\text{SR})_{18}$ NCs was according to our reported CO-reduction method.⁴⁵ Briefly, aqueous solutions of *p*-MBA (50 mM in 150 mM NaOH , 0.4 mL) and HAuCl_4 (40 mM, 0.25 mL) were mixed in 9.5 mL of ultrapure water under stirring (500 rpm). After 2 hours, the color of the reaction solution turned to light yellow, indicating that Au(III) ions were reduced to Au(I)-SR complexes. The solution pH was then brought to 11.6 and CO was bubbled through for 2 min. The flask was sealed airtight and the reaction was continued for 72 hours. The as-prepared $\text{Au}_{25}(\text{p-MBA})_{18}$ NCs were purified by ultrafiltration using 3 kDa cellulosic disk membrane several times to remove the remaining Au-(*p*-MBA) complexes and free *p*-MBA ligands before the catalytic measurements. The purified samples were also concentrated to 0.1 mM before use. The $\text{Au}_{25}(\text{p-MBA})_{18}$ NCs were characterized by UV-Vis absorption spectrometry (Shimadzu UV-1800 spectrometer). ESI-MS analysis was carried out on a Bruker microTOF-Q system in negative ion mode. Detailed operating conditions of ESI-MS analysis were: source temperature = 100 °C, dry gas flow rate = 4 L per min, nebulizer pressure = 2 bar and capillary voltage = 3.5 kV. In a typical ESI-MS analysis, 0.1 mL of sample was injected with a flow rate of 180 μL per hour. The Au content was determined by inductively coupled plasma mass spectrometry (ICP-OES) on an Agilent 7500A instrument.

Catalytic reaction

Catalytic measurement was done in 20 mL glass vial at room temperature and under atmospheric pressure with 500 rpm stirring speed. The catalyst ($\text{Au}_{25}(\text{p-MBA})_{18}$ NCs, 0.1 mM, 0.2 mL) was mixed with 4-nitrophenol (0.5 mM, 0.2 mL), leading to a $\text{Au}_{25}(\text{p-MBA})_{18}$ -to-(4-nitrophenol) molar ratio of 1 : 5. Then, NaBH_4 solution (~1.172 mM, 1.6 mL) was added into the mixture, leading to 25 \times more NaBH_4 than the stoichiometric requirement for the conversion of 4-nitrophenol into 4-aminophenol (similar to 4-nitrophenol-to- NaBH_4 molar ratio of 1 : 18.75 and $\text{Au}_{25}(\text{p-MBA})_{18}$ -to- NaBH_4 molar ratio of 1 : 93.75). Of note, this reaction condition was used throughout the study. For every time interval, 0.2 mL of sample was collected from the mixture for UV-Vis absorption analysis. Meanwhile, for ESI-MS analysis, 0.1 mL of sample was collected and injected into the instrument at a selected time interval. Detailed operating conditions of ESI-MS analysis were similar to those used for the characterization of $\text{Au}_{25}(\text{p-MBA})_{18}$ NCs.

3 Results and discussion

Hydrogenation of 4-nitrophenol in solution has been widely used as the model reaction for evaluating catalytic performance of Au nanocatalysts, especially of Au NPs.^{46–51} However, the catalytic mechanism of Au NPs for this reaction is still not

well understood due to the ill-defined structures of Au NPs, especially when most of them were polydisperse and immobilized on support materials. Hence, ligand-protected Au NCs could be attractive due to their atomic precision and well-defined structure. Herein, $\text{Au}_{25}(\text{p-MBA})_{18}$ was chosen as the model catalyst as this NC species has good stability in solution and it can be produced in a large scale with high purity.⁴⁵ The $\text{Au}_{25}(\text{p-MBA})_{18}$ NCs were synthesized according to a reported carbon monoxide (CO)-reduction method,⁴⁵ and the characterization of the purified clusters is shown in Fig. S1 (ESI[†]). We hypothesized that the structural transformation of $\text{Au}_{25}(\text{p-MBA})_{18}$ NCs would occur in solution if the NCs were unstable (and the ligands were dynamic on the surface of Au NCs) during and after the catalytic reaction. The stability of $\text{Au}_{25}(\text{p-MBA})_{18}$ NCs can be analyzed by monitoring one of the characteristic absorption peaks of Au₂₅ NCs (*i.e.*, ~690 nm) by UV-Vis absorption analysis. The stability can also be analyzed by monitoring the presence of $\text{Au}_{25}(\text{p-MBA})_{18}$ NCs by ESI-MS because this analytical instrument applies soft ionization technique that minimize the fragmentation of metallic molecules during measurement. ESI-MS has been widely used for study-

ing the growth mechanism of Au NCs.^{45,52–54} By using ESI-MS, all important species including the precursors, Au-ligand complexes and intermediate clusters can be successfully identified by comparing the intact molecular weight of the compounds and their simulated isotope patterns.⁵⁵

We first optimized the reaction conditions to ensure that the characteristic peaks of $\text{Au}_{25}(\text{p-MBA})_{18}$ at ~690 nm and the peak of 4-nitrophenolate ions at ~400 nm can be observed clearly under UV-Vis absorption spectrometry (Fig. 1a). Notably, a small amount of NaBH_4 (or a low concentration) is preferable for ESI-MS analysis because excessive inorganic ions (*e.g.*, Na^+ from NaBH_4) could disturb the ESI-MS measurement. However, the amount of NaBH_4 should be sufficient to activate the hydrogenation of 4-nitrophenol. Based on our optimization study (Fig. S2a–c[†]), the most suitable amount of NaBH_4 was 25 times that of the stoichiometric requirement (in stoichiometry, three moles of NaBH_4 are required to convert four moles of 4-nitrophenol to four moles of 4-aminophenol). In addition, a higher amount of NaBH_4 (more than 40 \times) is also unsuitable for this study because it could cause the formation of bigger Au NPs, which cannot be detected by ESI-MS analysis (Fig. S2[†]).

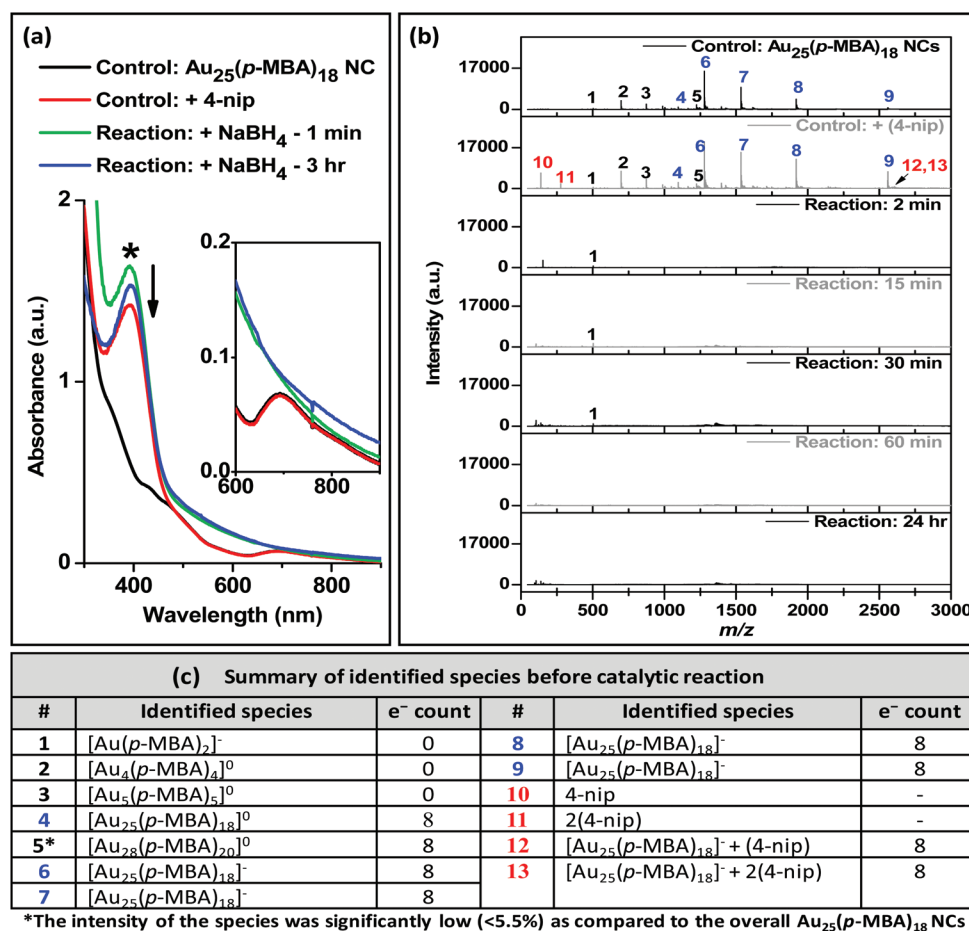


Fig. 1 Time evolution of 4-nitrophenol hydrogenation catalyzed by $\text{Au}_{25}(\text{p-MBA})_{18}$ NCs under (a) UV-Vis absorption analysis and (b) ESI-MS analysis. (c) The table shows the summary of identified species before the catalytic reaction. Detailed molecular formulas of the identified species and the validations of the representative species with the simulated isotope patterns are shown in Table S1 and Fig. S3.[†]

Under this optimized reaction condition, we observed a decreasing peak of 4-nitrophenolate ions at ~ 400 nm (symbolized as *) in the UV-Vis absorption spectra, which indicates that the conversion of 4-nitrophenol still occurred at this low concentration of NaBH_4 (Fig. 1a). The zoomed-in UV-Vis absorption spectra (inset, Fig. 1a) show the disappearance of the characteristic UV-Vis absorption peak of Au_{25} NCs at ~ 690 nm, which indicates that the $\text{Au}_{25}(\text{p-MBA})_{18}$ NCs were unstable and might undergo structural transformation during the catalytic reaction. Therefore, ESI-MS analysis is necessary to further determine the structural transformation of Au NCs during the catalytic reaction. Based on the ESI mass spectra in Fig. 1b, we could clearly observe several peaks for control experiments only (before the catalytic reaction). The major peaks are attributed to $\text{Au}_{25}(\text{p-MBA})_{18}$ NCs (Fig. 1b, #4, 6–9) and there are a few peaks of Au-(p-MBA) complexes (Fig. 1b, #1–3, 5).

When the $\text{Au}_{25}(\text{p-MBA})_{18}$ catalyst was mixed with 4-nitrophenol, we could still observe peaks for the NC catalysts (Fig. 1b, #4, 6–9). Moreover, we could also observe several additional peaks. These peaks were attributed to the adsorption of one or two 4-nitrophenol molecules on $\text{Au}_{25}(\text{p-MBA})_{18}$ NCs (Fig. 1b, #12 for the adsorption of one 4-nitrophenol and #13 for the adsorption of two 4-nitrophenol). These observations are consistent with our previous study,⁴⁰ although the molar ratios of $\text{Au}_{25}(\text{p-MBA})_{18}$ -to-4-nitrophenol in these two studies were different. Thus, it can be generalized that the adsorption of one and two 4-nitrophenol molecules is a common feature in the catalytic mechanism of 4-nitrophenol hydrogenation catalyzed by $\text{Au}_{25}(\text{p-MBA})_{18}$ NCs. The observations are consistent with the presence of free 4-nitrophenol monomers (Fig. 1b, #10, $m/z \sim 138$) and dimers (Fig. 1b, #11, $m/z \sim 277$) in the solution. The summary of all identified species (table, Fig. 1c) suggests that most of the Au NCs have eight valence electron counts, indicating a stable configuration of the superatomic $\text{Au}_{25}(\text{SR})_{18}$ NC.⁴ The ESI mass spectra in Fig. 1b also suggest that the $\text{Au}_{25}(\text{p-MBA})_{18}$ NCs were still stable after the adsorption of 4-nitrophenol; while they were unstable in the presence of NaBH_4 , as their peaks disappeared when the catalytic reaction was initiated by adding the NaBH_4 solution (Fig. 1b). However, it should be noted that the addition of NaBH_4 would increase the concentration of small inorganic ions (e.g., Na^+) in the reaction mixture, which could disturb the ESI-MS measurement by reducing the intensity of all peaks. Therefore, to identify the presence of Au NCs during the catalytic reaction, we had to zoom-in the ESI mass spectra.

Fig. 2 illustrates the results of ESI-MS analysis during the catalytic reaction. Several new species of Au NCs were identified, suggesting the occurrence of structural transformations of $\text{Au}_{25}(\text{p-MBA})_{18}$ NCs (Fig. 2a). These identified species are summarized in the table of Fig. 2c and they are grouped into the identified species after 2 and 15 minutes of reaction. In Fig. 2a, a peak of p-MBA ligands (#b, $m/z \sim 154$, $[\text{p-MBA} - \text{H}^{\dagger}]^{-}$) can be clearly seen at the beginning of the catalytic reaction, but it was not observed before the catalytic reaction

(Fig. 1b). The intensity of this peak (p-MBA ligands) decreased immediately and almost disappeared after 15 minutes of reaction, most probably due to the re-adsorption of the p-MBA ligands during the re-formation of $\text{Au}_{25}(\text{p-MBA})_{18}$ NCs and/or formation of new Au NCs. We also observed an increasing peak of the $\text{Au}(\text{p-MBA})_2$ complex (Fig. 2a, $m/z \sim 503$, #1, $[\text{Au}(\text{p-MBA})_2]^{-}$) at the beginning of catalytic reaction, which was further decreased after 15 minutes of reaction. The desorption and re-adsorption of the ligands imply that the ligands were dynamic during the catalytic reaction and might cause structural transformation of $\text{Au}_{25}(\text{p-MBA})_{18}$ NCs. This structural transformation of $\text{Au}_{25}(\text{p-MBA})_{18}$ NCs could also involve the detachment and re-attachment of $\text{Au}(\text{p-MBA})_2$ complexes.

In addition, we observed a mixture of smaller Au NCs (e.g., $\text{Au}_{23-25}(\text{p-MBA})_{14-17}$ NCs), which were denoted by a wide range of peaks (Fig. 2a, #d, m/z range of ~ 1433 to 1966) at the beginning of the catalytic reaction. These NC species might be formed through the removal of ligands and detachment of $\text{Au}(\text{p-MBA})_2$ complex from $\text{Au}_{25}(\text{p-MBA})_{18}$ NCs. The most dominant species of these smaller Au NCs were $[\text{Au}_{23}(\text{p-MBA})_{16}]^{-}$ NCs (ESI mass spectrum of a representative species with its simulated isotope pattern is shown in Fig. 2b, #d, $m/z \sim 1762$). Then, after 15 minutes of reaction, larger Au NCs were observed, and the most dominant species was $[\text{Au}_{26}(\text{p-MBA})_{19}]^0$ (ESI mass spectrum of a representative species with its simulated isotope pattern is shown in Fig. 2b, #i, $m/z \sim 1359.5$). Majority of the identified species after 15 minutes of reactions were quite stable even after 60 minutes of reaction. Some of them could be detected after 24 hours of reaction (Fig. S6[†]), indicating that the clusters did not decompose and grow into larger Au NPs; however, they were structurally transformed into other sizes of clusters after the catalytic reaction.

To gain a better understanding about the structural transformation of Au NCs during the catalytic reaction, the relative intensities of identified species over the reaction time were summarized in Fig. 3. Several important observations are related to the structural evolution of Au NCs. Firstly, the intensity of $\text{Au}_{25}(\text{p-MBA})_{18}$ NCs decreased exponentially during the catalytic reaction. Approximately 3% of the $\text{Au}_{25}(\text{p-MBA})_{18}$ NCs remained after 24 hours of reaction. Secondly, most of the $\text{Au}_{25}(\text{p-MBA})_{18}$ NCs were converted into smaller Au NCs (Au_{23} NCs) at the beginning of the catalytic reaction due to the detachment of p-MBA ligands and $\text{Au}(\text{p-MBA})_2$ complexes. The dominant species were $[\text{Au}_{23}(\text{p-MBA})_{16}]^{-}$ NCs. The conversion of Au_{25} NCs into Au_{23} NCs in the reductive environment (addition of NaBH_4) was also reported in a previous study.⁴³ However in this study, these small Au_{23} NCs were unstable in the catalytic mixture as their intensity decreased immediately after 15 minutes of reaction. Thus, they could be the intermediate clusters in the structural transformation of $\text{Au}_{25}(\text{p-MBA})_{18}$ NCs.

Thirdly, the desorption of p-MBA ligands at the beginning of catalytic reaction also caused the formation of $\text{Au}_{25}(\text{p-MBA})_{15-17}$ NCs. For example, Au_{25} NCs with fifteen p-MBA ligands (Table S2, #d2, $m/z \sim 1482$ –1493) and sixteen

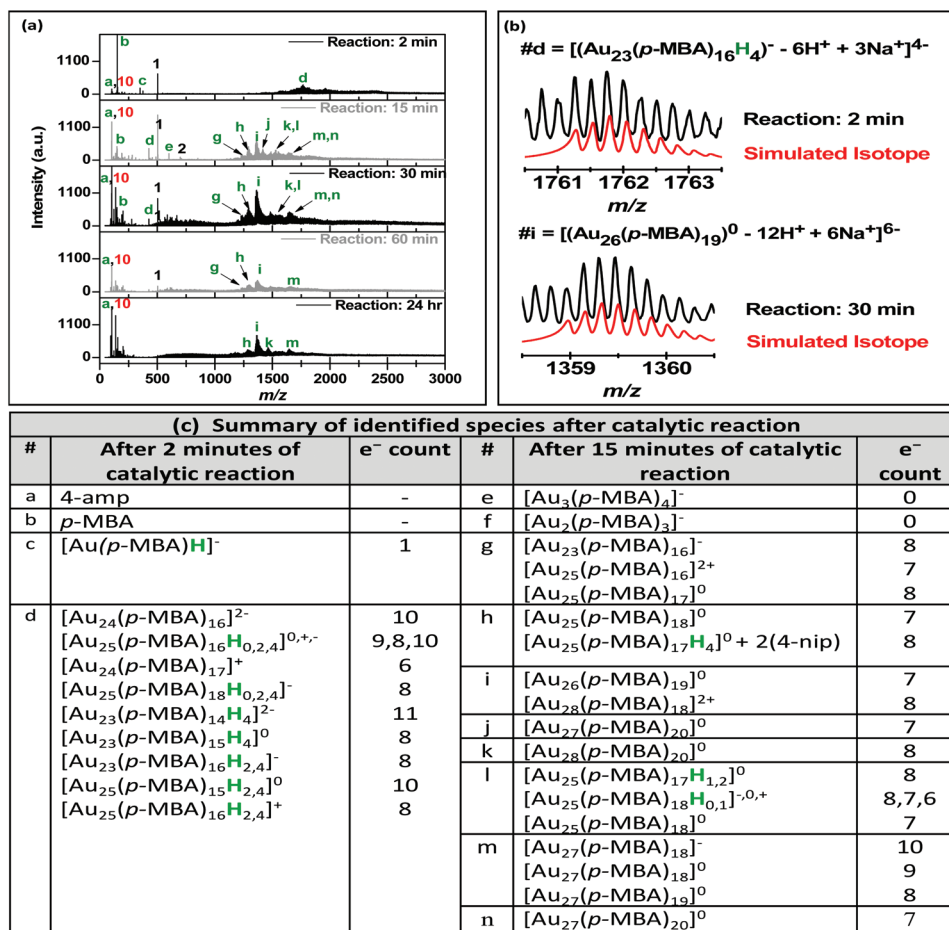


Fig. 2 (a) Zoomed-in ESI mass spectra during 4-nitrophenol hydrogenation catalyzed by Au₂₅(*p*-MBA)₁₈ NCs. (b) ESI mass spectra of two identified species with their simulated isotope patterns. (c) The table shows the summary of all identified species during the catalytic reaction. The detailed molecular formulas of the identified species after 2 minutes of reaction are tabulated in Table S2 and their validations with simulated isotope patterns are shown in Fig. S4.† The detailed molecular formulas of the identified species after 15 minutes of reaction are tabulated in Table S3 and their validations with simulated isotope patterns are shown in Fig. S5 and S6.† The detailed molecular formulas of identified species after 24 hours of reaction and their validations with simulated isotope patterns are shown in Fig. S7.†

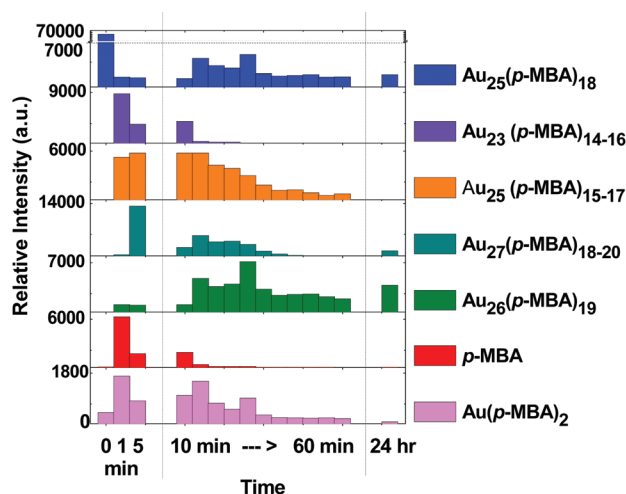


Fig. 3 Relative intensities of the major identified species of Au NCs, Au(*p*-MBA)₂ complexes and *p*-MBA ligands (from ESI-MS data) over the reaction time.

p-MBA ligands (Table S2, #d3,† *m/z* ~ 1500–1510) were observed. Since the intensities of these NCs peaks decreased over time and fully disappeared after 24 hours of reaction, they could also be considered as the intermediate clusters. Finally, after the disappearance of the smaller Au₂₃ NCs, the major identified species were Au₂₅(*p*-MBA)₁₈ and larger Au_{26–27} NCs. The dominant species were Au₂₆(*p*-MBA)₁₉ NCs (Fig. 2b, #i and Table S3, #i1,† *m/z* ~ 1556–1567), which were stable even after 24 hours of reaction (Fig. S7, #i1†). Au₂₆(*p*-MBA)₁₉ is a new stable Au NC species in solution, which has not been reported in previous studies. The proposed structural transformation of Au₂₅(*p*-MBA)₁₈ NCs during the catalytic reaction is summarized in Fig. 4. It is worth noting that the desorption of Au(*p*-MBA)₂ complexes could also form Au₂₄ NCs in the solution, similar to when we observed [Au₂₄(*p*-MBA)₁₆]²⁻ at the beginning of catalytic reaction (Table S2 and Fig. S4, #d1,† *m/z* ~ 1422–1445).

Fascinated by the ligand dynamic and structural transformation of Au₂₅(*p*-MBA)₁₈ NC, we further investigated the factors

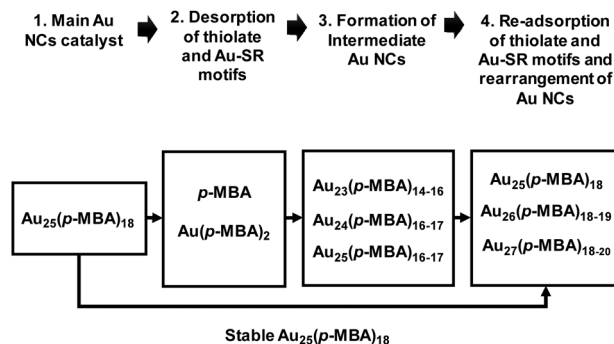


Fig. 4 Proposed structural transformations of Au NCs during 4-nitrophenol hydrogenation in solution.

causing these phenomena during the catalytic reaction. The results in Fig. S8[†] show that NaBH₄ was the main factor that induced the ligand dynamic and structural transformation of Au₂₅(*p*-MBA)₁₈ NCs during the hydrogenation of 4-nitrophenol in solution as compared to 4-nitrophenol (even at a molar ratio of two times higher than NaBH₄) and pH of the solution. This finding is consistent with a previous study reporting that a chemical stripping by the addition of NaBH₄ could remove the protecting ligands at mild conditions.⁵⁶

However, in catalysis, the effects of NaBH₄ could be more than just removing the ligands and exposing more Au active sites. As gold catalyst is a good electron mediator for most hydrogenation reactions, the hydrides (from the hydrolysis of NaBH₄ in solution) will bond to Au surface, forming Au-H active sites that are more reactive and donate electrons for the hydrogenation of 4-nitrophenol to 4-aminophenol.⁵⁷ The Au-H

bond could be formed through the high affinity of hydride (H⁻) towards Au(I) at the staple motifs or on the surface of Au core. However, experimental evidence for the adsorption of hydrides on Au nanocatalysts was rarely reported, probably due to the difficulties in probing the adsorption of small hydrides on the ill-defined Au NPs or on the supported Au NCs. Only a few studies have reported the experimental evidence for an Au-H bond on the surface of Au catalysts. For example, the formation of Au-H species on the surface of Au NPs supported on cerium oxides was evidenced using inelastic neutron scattering.⁵⁸ Therefore, in this study, we had carefully analyzed the ESI mass spectra of the catalytic reaction.

Interestingly, we observed the adsorption of hydrides (labeled with green H) on some of the identified Au NCs from our ESI-MS data (Fig. 5). Most of them were identified at the beginning of catalytic reaction. An example of hydride adsorption on Au₂₃ NCs is the [(Au₂₃(*p*-MBA)₁₆H₄)⁻ - 6H⁺ + 3Na⁺]⁴⁻ ion (Fig. 5, #d9, *m/z* ~ 1762). Meanwhile, an example of hydride adsorption on Au₂₅ NCs is the [(Au₂₅(*p*-MBA)₁₈H₂)⁻ - 9H⁺ + 5Na⁺]⁵⁻ ion (Fig. 5, #d4, *m/z* ~ 1558). We also observed hydrides bonded to the Au(I)-(*p*-MBA) complexes (e.g., [Au(*p*-MBA)H]⁻, Fig. 5, #c, *m/z* ~ 351). It can be speculated that the hydride had replaced one of the *p*-MBA ligands of the [Au(*p*-MBA)₂]⁻ complex. Likewise, the replacement of ligands was observed in Au₂₅ NCs (Table S3, #11,† *m/z* ~ 1518, [(Au₂₅(*p*-MBA)₁₇H)⁰ - 8H⁺ + 3Na⁺]⁵⁻). The observations convey that the hydrides not only induce desorption of *p*-MBA ligands (leading to the formation of more reactive Au-H sites), but also behave as ligands to maintain the structures of the clusters.

A number of studies on metal-hydride active sites in catalysis have been reported, specifically in the catalytic application

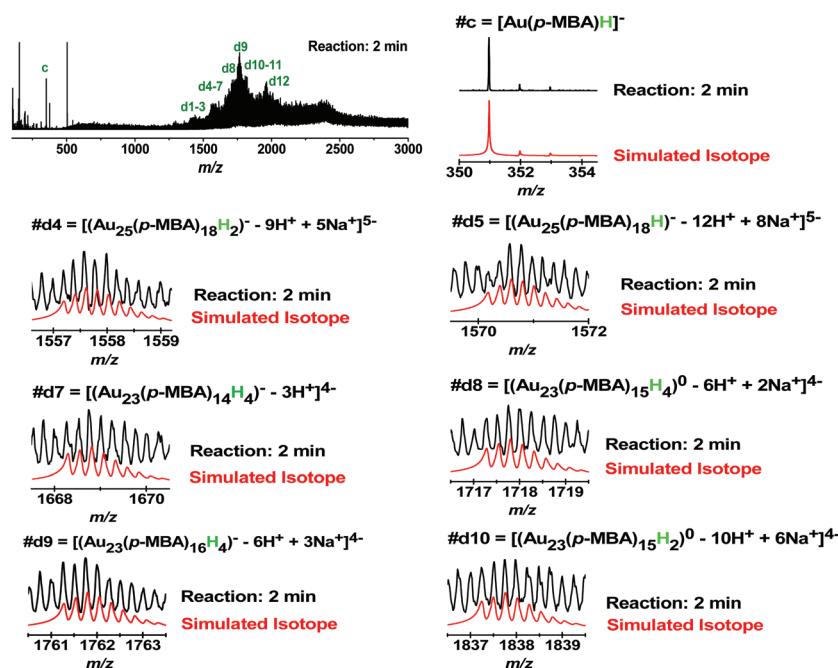


Fig. 5 Some examples of Au NCs with hydrides adsorption (identified at the beginning of catalytic reaction).

of homogeneous metal–ligand complex catalysts.^{59–61} Only recently, metal-hydrides on metal NCs has been highlighted in several reported studies, where the hydrides could serve as the protecting ligands and active sites for catalysis.^{62–64} For instance, silver NCs with hydrides-rich ligands have been synthesized and characterized.^{62,64} A recent study also reported that the Cu–H sites of copper-hydride NCs were important for the catalytic activity and selectivity of the clusters in electrochemical CO₂ reduction.⁶³ Therefore, the experimental evidence showing hydrides adsorption on Au NCs, as provided in this study, could benefit the understandings of the metal-hydride active sites of Au NCs in catalysis.

Based on the well-known structure of homogeneous ligand-protected Au₂₅(SR)₁₈, the hydride adsorption could be on the Au(I) on the surface of Au core and/or on the low-coordinated Au(I) at the staple motifs, as illustrated in Fig. S9.† It can be speculated that hydrides would favor adsorption at the low-coordinated Au(I) at staple motifs due to the presence of more Au(I) species within the staple motifs. In addition, based on the reported DFT calculation, the hydride addition to Au(I)–SR oligomers (staple motifs) would yield free thiols (*via* desorption of thiolate ligands) during the growth of thiolate-protected Au NPs, which is favorable in water and might not be favorable in gas phase and organic solvent.⁶⁵ Similar cases were observed in our study when the hydrogenation of 4-nitrophenol was performed in an aqueous solution, catalyzed by the water-soluble Au₂₅(*p*-MBA)₁₈ NCs. However, we cannot exclude the concurrent adsorption of hydrides on the surface of Au core of the Au NCs.

Based on above observations, we propose a possible catalytic mechanism of Au₂₅(*p*-MBA)₁₈ NCs during 4-nitrophenol hydrogenation in solution. A classical catalyst would not be consumed during the catalytic reaction. However, for Au NC catalysis, the structural transformation of Au NC catalysts can occur during the catalytic reaction, thus affecting the final structure of the catalysts and leading to the formation of intermediate clusters (which could also be catalytically active). Therefore, several catalytically active Au NCs could exist in the solution during the hydrogenation of 4-nitrophenol. The proposed catalytic mechanism suggests that Au₂₅(*p*-MBA)₁₈ could undergo any of the following three pathways during the hydrogenation of 4-nitrophenol in solution (Fig. 6).

In the first pathway (red arrows, Fig. 6), the Au₂₅(*p*-MBA)₁₈ NCs undergo structural transformation into Au₂₄(*p*-MBA)_{16–17} and Au₂₃(*p*-MBA)_{14–16} (of which Au₂₃(*p*-MBA)₁₆ is the major species). Then, these smaller NCs were transformed back to Au₂₅(*p*-MBA)₁₈ or larger Au NCs (of which Au₂₆(*p*-MBA)₁₉ is the major species). As most of the smaller Au NCs showed hydride adsorption, they could also be catalytically active for 4-nitrophenol hydrogenation. The transformation of Au NCs could also be a side reaction in the hydrogenation of 4-nitrophenol catalyzed by homogeneous Au NCs, which consumes electrons and hydrides from NaBH₄. This analysis justifies why an excess amount of NaBH₄ is required to activate the catalytic reaction of 4-nitrophenol hydrogenation using ligand-protected Au NC catalysts.

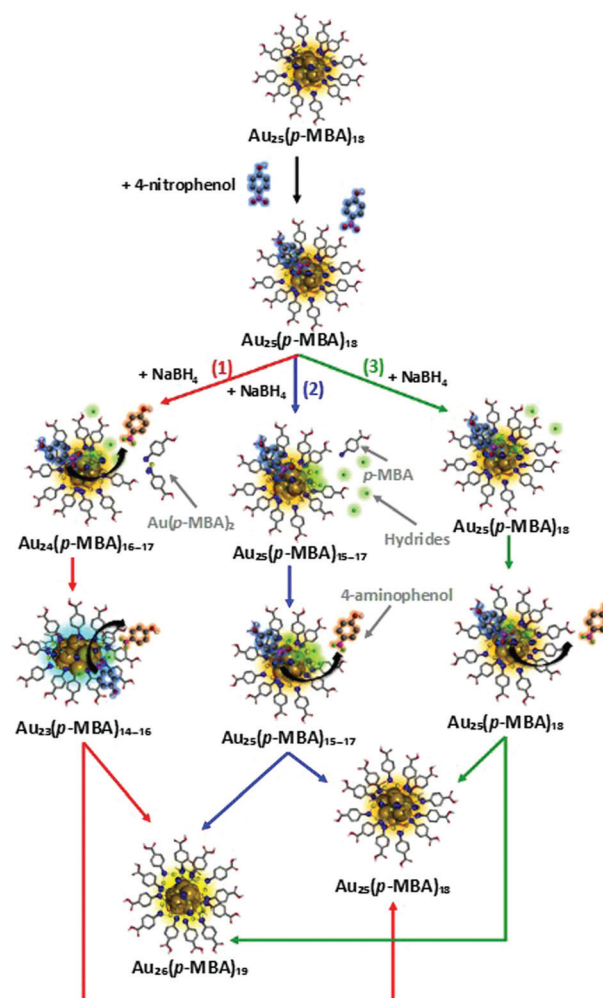


Fig. 6 Proposed catalytic mechanisms of Au₂₅(*p*-MBA)₁₈ for 4-nitrophenol hydrogenation in solution.

In the second pathway (blue arrows, Fig. 6), the hydride adsorption causes the desorption of *p*-MBA ligands and the catalytic reaction could occur on these Au₂₅ NCs because they have more exposed Au active sites due to the removal of ligands (*e.g.*, Au₂₅(*p*-MBA)_{15–17} NCs). These Au NCs had better exposure of the middle layer active sites (surface of Au core) as compared to their parental Au₂₅(*p*-MBA)₁₈ NCs, therefore they could be more reactive for the catalytic reaction. After 24 hours of reaction, these Au₂₅(*p*-MBA)_{15–17} NCs might undergo structural transformation into neutrally charged [Au₂₅(*p*-MBA)₁₈]⁰ NCs or larger Au NCs (the dominant species is [Au₂₆(*p*-MBA)₁₉]⁰).

The third pathway (green arrows, Fig. 6) involves the entire Au₂₅(*p*-MBA)₁₈ cluster as the active catalyst because the adsorption of 4-nitrophenol was observed mainly on Au₂₅(*p*-MBA)₁₈. Also, we can still observe a few stable Au₂₅(*p*-MBA)₁₈ NCs from the beginning till 24 hours of the catalytic reaction (Fig. 4 and Fig. S7†). Some of these Au₂₅(*p*-MBA)₁₈ NCs also exhibited hydride adsorption (*e.g.*, Fig. 5, #d5, *m/z* ~ 1571, [(Au₂₅(*p*-MBA)₁₈H)[−] − 12H⁺ + 8Na⁺]^{5−}). After 24 hours of reac-

tion, the hydride adsorption on $\text{Au}_{25}(\text{p-MBA})_{18}$ NCs was not observed but the clusters had neutral charge ($[\text{Au}_{25}(\text{p-MBA})_{18}]^0$ (Fig. S7, #h1†) with seven valence electron counts (one of the electrons probably had been donated to the catalytic reaction). Of note, we cannot exclude that the free $\text{Au}(\text{p-MBA})_2$ complexes could also be one of the active species for the catalytic reaction as we also observed the Au–H species in the complexes, but the intensity of these species was low, and they were only available at the beginning of catalytic reaction. Therefore, it can be speculated that the $[\text{Au}(\text{p-MBA})\text{H}]^-$ complexes would mainly participate in the structural transformation of Au NCs rather than in the catalytic reaction.

Adsorption of any hydride or 4-nitrophenol on $[\text{Au}_{26}(\text{p-MBA})_{19}]^0$ NCs was not observed. Therefore, it is quite difficult to claim that these newly formed Au NCs were catalytically active for the hydrogenation reaction. We can only speculate that $[\text{Au}_{26}(\text{p-MBA})_{19}]^0$ NCs can be catalytically active if $[\text{Au}_{26}(\text{p-MBA})_{19}]^0$ was originally carrying a negative charge ($[\text{Au}_{26}(\text{p-MBA})_{19}]^-$) with eight valence electron counts; but due to the catalytic reaction, one of the electrons was donated for the hydrogenation of 4-nitrophenol leading to the formation of neutral $[\text{Au}_{26}(\text{p-MBA})_{19}]^0$ species with seven valence electron counts. It should be noted that the structural transformation of Au NCs also depends on the amount of NaBH_4 . Different amount of NaBH_4 may cause the formation of different Au NCs during the catalytic reaction.

4 Conclusions

We had monitored the hydrogenation of 4-nitrophenol catalyzed by $\text{Au}_{25}(\text{p-MBA})_{18}$ NCs using real-time ESI-MS, which discloses the occurrence of ligand dynamic and structural transformation phenomena of the catalyst during the solution-based catalytic reaction. The atomic precision of the ligand-protected Au NCs has enabled us to explore the ligand dynamic and structural transformation of the catalyst, thus providing insights into the stability, active species and catalytic mechanism of $\text{Au}_{25}(\text{p-MBA})_{18}$ NCs at molecular level. It was also found that the adsorption of hydrides induced ligand desorption and structural transformation of Au NCs, which could be a side reaction in 4-nitrophenol hydrogenation catalyzed by Au NCs; therefore, an excess amount of NaBH_4 is required to activate the hydrogenation of 4-nitrophenol. The presence of metal-hydride (Au–H) species on the surface of the Au NC catalysts will also enhance the electron transfer and improve the efficiency of catalysts for the hydrogenation reaction. This study may expand the scope of metal NCs in catalysis, as the hydride-protected metal NCs have been an interesting topic for catalysis research.

Conflicts of interest

There are no conflicts to declare.

Acknowledgements

This study was financially supported by the Ministry of Education, Singapore, under the Grant of R-279-000-481-112.

Notes and references

- 1 T. Laaksonen, V. Ruiz, P. Liljeroth and B. M. Quinn, *Chem. Soc. Rev.*, 2008, **37**, 1836–1846.
- 2 R. W. Murray, *Chem. Rev.*, 2008, **108**, 2688–2720.
- 3 M. Zhu, C. M. Aikens, M. P. Hendrich, R. Gupta, H. Qian, G. C. Schatz and R. Jin, *J. Am. Chem. Soc.*, 2009, **131**, 2490–2492.
- 4 R. Jin, C. Zeng, M. Zhou and Y. Chen, *Chem. Rev.*, 2016, **116**, 10346–10413.
- 5 H. Chong and M. Zhu, *ChemCatChem*, 2015, **7**, 2296–2304.
- 6 Y. Zhu, H. Qian, B. A. Drake and R. Jin, *Angew. Chem., Int. Ed.*, 2010, **49**, 1295–1298.
- 7 P. Liu, R. Qin, G. Fu and N. Zheng, *J. Am. Chem. Soc.*, 2017, **139**, 2122–2131.
- 8 B. Zhang, J. Fang, J. Li, J. J. Lau, D. Mattia, Z. Zhong, J. Xie and N. Yan, *Chem. – Asian J.*, 2016, **11**, 532–539.
- 9 J. Fang, J. Li, B. Zhang, X. Yuan, H. Asakura, T. Tanaka, K. Teramura, J. Xie and N. Yan, *Nanoscale*, 2015, **7**, 6325–6333.
- 10 Y. Liu, H. Tsunoyama, T. Akita, S. Xie and T. Tsukuda, *ACS Catal.*, 2011, **1**, 2–6.
- 11 L. Li, S. Huang, J. Song, N. Yang, J. Liu, Y. Chen, Y. Sun, R. Jin and Y. Zhu, *Nano Res.*, 2016, **9**, 1182–1192.
- 12 Y. Zhu, H. Qian, M. Zhu and R. Jin, *Adv. Mater.*, 2010, **22**, 1915–1920.
- 13 Y. Zhu, H. Qian and R. Jin, *Chem. – Eur. J.*, 2010, **16**, 11455–11462.
- 14 P. Huang, G. Chen, Z. Jiang, R. Jin, Y. Zhu and Y. Sun, *Nanoscale*, 2013, **5**, 3668–3672.
- 15 C. Liu, S. Lin, Y. Pei and X. C. Zeng, *J. Am. Chem. Soc.*, 2013, **135**, 18067–18079.
- 16 H. Tsunoyama, H. Sakurai, Y. Negishi and T. Tsukuda, *J. Am. Chem. Soc.*, 2005, **127**, 9374–9375.
- 17 J. Good, P. N. Duchesne, P. Zhang, W. Koshut, M. Zhou and R. C. Jin, *Catal. Today*, 2017, **280**, 239–245.
- 18 G. Ma, A. Binder, M. Chi, C. Liu, R. Jin, D.-e. Jiang, J. Fan and S. Dai, *Chem. Commun.*, 2012, **48**, 11413–11415.
- 19 X. Nie, H. Qian, Q. Ge, H. Xu and R. Jin, *ACS Nano*, 2012, **6**, 6014–6022.
- 20 X. Nie, C. Zeng, X. Ma, H. Qian, Q. Ge, H. Xu and R. Jin, *Nanoscale*, 2013, **5**, 5912–5918.
- 21 Z. Wu, D.-e. Jiang, A. K. P. Mann, D. R. Mullins, Z.-A. Qiao, L. F. Allard, C. Zeng, R. Jin and S. H. Overbury, *J. Am. Chem. Soc.*, 2014, **136**, 6111–6122.
- 22 K. Zheng, M. I. Setyawati, T.-P. Lim, D. T. Leong and J. Xie, *ACS Nano*, 2016, **10**, 7934–7942.
- 23 O. Lopez-Acevedo, K. A. Kacprzak, J. Akola and H. Häkkinen, *Nat. Chem.*, 2010, **2**, 329–334.

- 24 X. Kong, H. Zhu, C. Chen, G. Huang and Q. Chen, *Chem. Phys. Lett.*, 2017, **684**, 148–152.
- 25 Z. M. Li, C. Liu, H. Abroshan, D. R. Kauffman and G. Li, *ACS Catal.*, 2017, **7**, 3368–3374.
- 26 G. Li, H. Qian and R. Jin, *Nanoscale*, 2012, **4**, 6714–6717.
- 27 G. Li, C. Liu, Y. Lei and R. Jin, *Chem. Commun.*, 2012, **48**, 12005–12007.
- 28 H. Abroshan, G. Li, J. Lin, H. J. Kim and R. Jin, *J. Catal.*, 2016, **337**, 72–79.
- 29 G. Li, D.-e. Jiang, C. Liu, C. Yu and R. Jin, *J. Catal.*, 2013, **306**, 177–183.
- 30 S. Zhao, A. Das, H. Zhang, R. Jin, Y. Song and R. Jin, *Prog. Nat. Sci.*, 2016, **26**, 483–486.
- 31 M. Dasog, W. Hou and R. W. J. Scott, *Chem. Commun.*, 2011, **47**, 8569–8571.
- 32 J. Li, R. R. Nasaruddin, Y. Feng, J. Yang, N. Yan and J. Xie, *Chem. – Eur. J.*, 2016, **22**, 14816–14820.
- 33 H. Chong, P. Li, J. Xiang, F. Fu, D. Zhang, X. Ran and M. Zhu, *Nanoscale*, 2013, **5**, 7622–7628.
- 34 G. Li and R. Jin, *J. Am. Chem. Soc.*, 2014, **136**, 11347–11354.
- 35 Y. Zhu, Z. Wu, C. Gayathri, H. Qian, R. R. Gil and R. Jin, *J. Catal.*, 2010, **271**, 155–160.
- 36 G. Li, H. Abroshan, Y. Chen, R. Jin and H. J. Kim, *J. Am. Chem. Soc.*, 2015, **137**, 14295–14304.
- 37 G. Li, C. Zeng and R. Jin, *J. Am. Chem. Soc.*, 2014, **136**, 3673–3679.
- 38 S. Zhao, R. X. Jin, H. Abroshan, C. J. Zeng, H. Zhang, S. D. House, E. Gottlieb, H. J. Kim, J. C. Yang and R. C. Jin, *J. Am. Chem. Soc.*, 2017, **139**, 1077–1080.
- 39 Q. Wang, L. Wang, Z. Tang, F. Wang, W. Yan, H. Yang, W. Zhou, L. Li, X. Kang and S. Chen, *Nanoscale*, 2016, **8**, 6629–6635.
- 40 R. R. Nasaruddin, T. Chen, J. Li, N. Goswami, J. Zhang, N. Yan and J. Xie, *ChemCatChem*, 2018, **10**, 395–402.
- 41 H. Yamamoto, H. Yano, H. Kouchi, Y. Obora, R. Arakawa and H. Kawasaki, *Nanoscale*, 2012, **4**, 4148–4154.
- 42 T. Higaki, C. Liu, Y. Chen, S. Zhao, C. Zeng, R. Jin, S. Wang, N. L. Rosi and R. Jin, *J. Phys. Chem. Lett.*, 2017, **8**, 866–870.
- 43 Y. Song, H. Abroshan, J. Chai, X. Kang, H. J. Kim, M. Zhu and R. Jin, *Chem. Mater.*, 2017, **29**, 3055–3061.
- 44 T. A. Dreier, O. A. Wong and C. J. Ackerson, *Chem. Commun.*, 2015, **51**, 1240–1243.
- 45 Z. Luo, V. Nachammai, B. Zhang, N. Yan, D. T. Leong, D. Jiang and J. Xie, *J. Am. Chem. Soc.*, 2014, **136**, 10577–10580.
- 46 P. Zhao, X. Feng, D. Huang, G. Yang and D. Astruc, *Coord. Chem. Rev.*, 2015, **287**, 114–136.
- 47 M. M. Nigra, J.-M. Ha and A. Katz, *Catal. Sci. Technol.*, 2013, **3**, 2976–2983.
- 48 A. A. Ismail, A. Hakki and D. W. Bahnemann, *J. Mol. Catal. A: Chem.*, 2012, **358**, 145–151.
- 49 H. Guo, Y. Ren, Q. Cheng, D. Wang and Y. Liu, *Catal. Commun.*, 2017, **102**, 136–140.
- 50 C. Li, P. Wang, Y. Tian, X. Xu, H. Hou, M. Wang, G. Qi and Y. Jin, *ACS Catal.*, 2017, **7**, 5391–5398.
- 51 S. Sharma, P. J. Bora, M. Boruah and S. K. Dolui, *Adv. Polym. Technol.*, 2015, **36**, 301–308.
- 52 Y. Yu, Z. Luo, Y. Yu, J. Y. Lee and J. Xie, *ACS Nano*, 2012, **6**, 7920–7927.
- 53 M. Krstic, A. Zavras, G. N. Khairallah, P. Dugourd, V. Bonacic-Koutecky and R. A. J. O'Hair, *Int. J. Mass Spectrom.*, 2017, **413**, 97–105.
- 54 M. R. Ligare, G. E. Johnson and J. Laskin, *Phys. Chem. Chem. Phys.*, 2017, **19**, 17187–17198.
- 55 T. Chen, Z. Luo, Q. Yao, A. X. H. Yeo and J. Xie, *Chem. Commun.*, 2016, **52**, 9522–9525.
- 56 S. Das, A. Goswami, M. Hesari, J. F. Al-Sharab, E. Mikmeková, F. Maran and T. Asefa, *Small*, 2014, **10**, 1473–1478.
- 57 M. A. Koklioti, T. Skaltsas, Y. Sato, K. Suenaga, A. Stergiou and N. Tagmatarchis, *Nanoscale*, 2017, **9**, 9685–9692.
- 58 I. P. Silverwood, S. M. Rogers, S. K. Callear, S. F. Parker and C. R. A. Catlow, *Chem. Commun.*, 2016, **52**, 533–536.
- 59 H. Ito, T. Saito, T. Miyahara, C. Zhong and M. Sawamura, *Organometallics*, 2009, **28**, 4829–4840.
- 60 C. A. Gaggioli, L. Belpassi, F. Tarantelli, D. Zuccaccia, J. N. Harvey and P. Belanzoni, *Chem. Sci.*, 2016, **7**, 7034–7039.
- 61 A. J. Jordan, G. Lalic and J. P. Sadighi, *Chem. Rev.*, 2016, **116**, 8318–8372.
- 62 M. S. Bootharaju, R. Dey, L. E. Gevers, M. N. Hedhili, J. M. Basset and O. M. Bakr, *J. Am. Chem. Soc.*, 2016, **138**, 13770–13773.
- 63 Q. Tang, Y. Lee, D. Y. Li, W. Choi, C. W. Liu, D. Lee and D. E. Jiang, *J. Am. Chem. Soc.*, 2017, **139**, 9728–9736.
- 64 M. Krstić, A. Zavras, G. N. Khairallah, P. Dugourd, V. Bonačić-Koutecký and R. A. J. O'Hair, *Int. J. Mass Spectrom.*, 2017, **413**, 97–105.
- 65 B. M. Barngrover and C. M. Aikens, *J. Phys. Chem. Lett.*, 2011, **2**, 990–994.